Airborne Optical Remote Sensing of Ocean Currents

Steven P. Anderson
Seth Zuckerman
Environmental Intelligence Group
Areté Associates
1550 Crystal Dr., Suite 703
Arlington, VA 22202

Shejun Fan
Jan van Smirren
Fugro GEOS
P O Box 740010
6100 Hillcroft (77081)
Houston, Texas 77274

Abstract— **This paper reports on the first data collections with the Remote Ocean Current Imaging System (ROCIS). ROCIS exploits time-space processing of airborne ocean wave imagery to produce maps of surface currents. These results demonstrate that the optical imaging technique has the potential to provide accurate (5 cm s^{-1}) surface current data over large areas both rapidly and cost effectively and complements traditional ocean survey approaches. This unique capability provides maps of current vectors on 250m x 250m (or finer) grids across a 3 km swath along the flight path. ROCIS may enable new understanding of ocean processes and be employed to provide improved regional ocean forecasts during a spill response.**

I. INTRODUCTION

Ocean surface currents play a primary role in determining the movement and dispersion of oil. During spill response, accurate and timely observations of ocean currents are of critical importance for spill planning, containment, monitoring, and recovery operations. The ocean varies on a broad range of temporal and spatial scales and it is important to use the type of measurement system best suited to a specific application.

Many measurements systems are presently employed in the continental shelf to monitor ocean currents. Satellite remote sensing provides estimates of ocean currents using feature tracking algorithms or satellite altimetry [1, 2]. Satellites provide a view of the largest scale features but cannot be relied on to provide timely and precise observations of the sea surface due to cloud cover or limited coverage coupled with sensor resolution. Drifting buoys have proven to be a cost effective means of collecting ocean current observations; however, the Lagrangian drifters often move out of the region of interest [3]. Acoustic Doppler Current Profilers (ADCP) mounted on moorings and platforms can provide real-time current information but are not always optimally located to aid with ocean prediction [4]. H/F Radar systems deployed along the coast or from offshore structures have shown some operational utility to the deepwater industry but only provide radial current information (unless deployed in pairs) and have limited resolution and range [5].

Shipboard ADCPs collect ocean current profiles while underway providing synoptic ocean circulation data. Traditionally these systems have been hull mounted on research vessels, mounted on poles placed over the side or towed behind vessels of opportunity [6]. The ships can operate both day and night and real-time data collection is limited primarily by weather and sea-state.

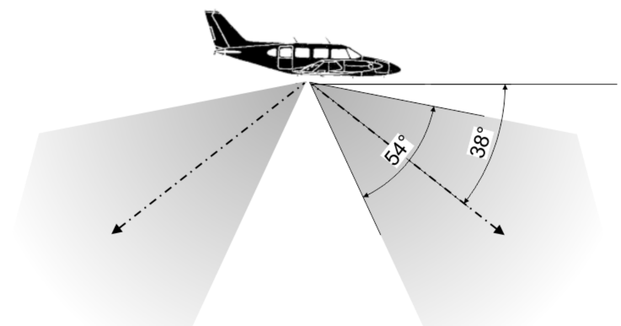

Figure 1. Remote Ocean Current Imaging System (ROCIS). An aircraft is equipped with a pair of 8 megapixel panchromatic cameras to image the waves on the water surface and measure surface currents. Cameras are aimed fore and aft to assure at least one camera is clear of sun glint. The focal lengths and grazing angles are configured to support flight altitudes from 3,000 to 10,000 feet. An inertial navigation system (INS) on the aircraft provides geo-referencing information.

Shipboard ADCP surveys are routinely used to supplement other measurement systems during critical offshore operations and several commercial service providers offer this capability. ADCP technology, at over 40 years old, is mature. However, surveying by ship is not always an ideal solution. First, mobilization and transit times can create a lag of several days (or more) before data collection begins. Second, ship speed is limited to 4-8 knots (depending on sea-state and installation details) thus limiting the coverage area and preventing multiple areas of interest to be mapped due to transit times between them, unless more than one vessel is used. The vessels speed also prevents a synoptic assessment of mesoscale features such as the Loop Current. This sparseness of data coverage limits its suitability for initializing numerical models. In addition to the lost time and cost associated with vessel mobilization, the necessity for refueling, resupplying and crew changes further reduces efficiency. Finally, in an oil spill scenario there is the potential for exposure of ship's crews to harmful volatile hydrocarbons.

978-0-933957-40-4 ©2013 MTS

Here we report on a new airborne current measurement capability that leverages recent advances in remote sensing: the Remote Ocean Current Imaging System (ROCIS) (**Figure 1**). ROCIS provides a cost effective and rapid response solution for the provision of surface current surveys over large offshore regions.

Section II describes the passive remote sensing technique employed to measure the surface currents. Section III reviews the field collections and results. A discussion and conclusions are presented in Section IV and Section V.

II. TECHNOLOGY

Prior work has demonstrated that airborne time-series imaging systems can remotely sense near-shore ocean currents [10]. The fundamental approach employs passive optics to image the surface waves and retrieve the currents from the observed Doppler shift. For this technique, adequate dwell (observation interval) and removal of aircraft motion is fundamental to accurate surface current retrievals. ROCIS expands earlier work, and simplifies the imaging hardware, allowing for compact hardware suitable for offshore applications.

A. Current Retrieval Algorithm

The motion of deepwater surface waves is described by the linear dispersion relationship (**Figure 2**). Longer waves move faster than shorter waves and all the waves will feel a Doppler shift from the mean surface current. Note, the only free parameter in this formulation is the current vector and it is this dispersion relationship that is exploited to retrieve the surface currents. This technique has proven to be successful in littoral and estuarine regions [11].

The first step in the current retrieval process is mapping the images to the water surface in a geographic reference frame. This requires an Inertial Navigation System (INS) to determine absolute camera location and orientation and knowledge of the absolute water elevation.

Next, an image stack is created by extracting sub-images or "patches" (typically 250m x 250m) around a fixed geographic location on the water surface. This creates the space/time information of the surface waves for that location (**Figure 3**). A three dimensional Fourier transform of the image stack is performed and the power spectral density (3D-PSD) is calculated (**Figure 4**).

The wave dispersion equation is then fit to the observed 3D-PSD using least-squares fitting to derive both components of the current for that patch of water. In addition, the goodness-of-fit and the signal-to-noise estimates are used to provide an error-metric: a quantitative estimate of uncertainty for the retrieval for the patch. Note the cameras image a broad band of ocean waves (4m to 100m) which allows for quite precise current estimation under a large range of wind speeds and sea-states.

B. ROCIS Imaging System

Earlier R&D imaging systems [10, 11] used a positioner to aim the cameras at a specific location on the water. This allowed for unlimited image dwell (the length of time that

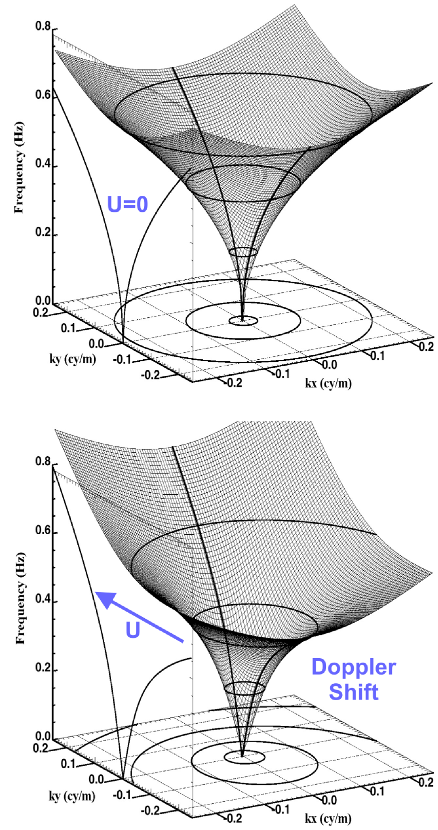

Figure 2. The motion of deep water surface waves can be approximated by the linear dispersion relationship:

$$\omega = \sqrt{g\kappa} + \kappa \cdot U$$

where ω is the wave frequency, κ is the vector wavenumber, g is the acceleration of gravity and U is the vector current. Shown is the dispersion surface for the case of no currents (top) and case of currents (bottom). The currents will Doppler shift the dispersion surface resulting in a tilted surface.

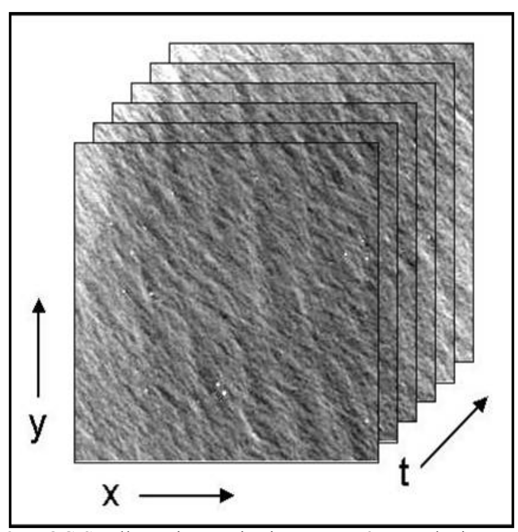

Figure 3. ROCIS collects time-series imagery at 2 Hz. The images are mapped to geographic coordinates on the water surface using the INS information. The result is an image stack of the surface waves [11].

(a)

(b)

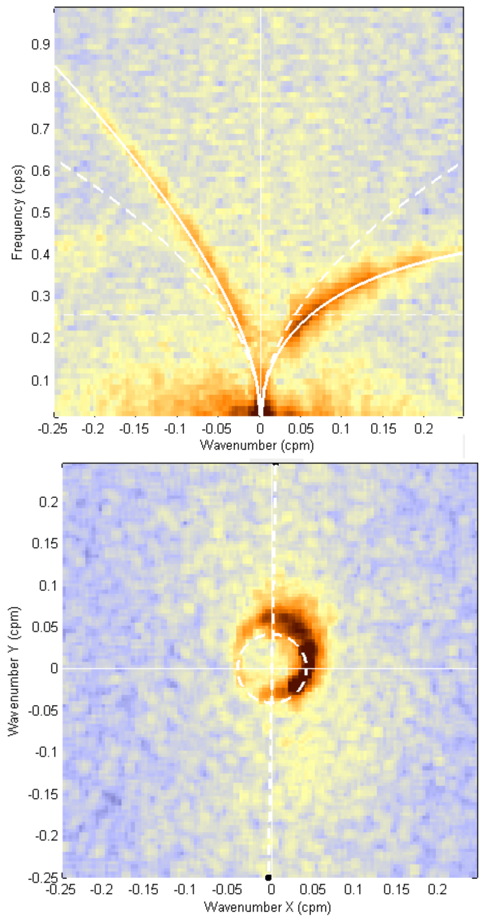

Figure 4. Power Spectral Density field from an image stack. This figure shows (a) a wavenumber slice in the direction of the current vector and (b) a frequency slice at 0.25Hz. Color shading indicates the energy level. The dashed line indicates the wave dispersion relation in the absence of currents. The dispersion surface is least-squares fit (solid line) to the observed PSD resulting in a current extraction (0.90 m s^{-1}.)

wave images are collected) as the aircraft circles over the target. The length of the dwell is important because it sets the wave frequency bandwidth and resolution.

The ROCIS system exploits a high resolution camera with a wide field of view that is fixed to the airframe. This allows for imaging a large surface area and the required dwell is obtained while flying a straight line. The system processes current retrievals for consecutive patches of water to generate continuous currents along the flight path in a "strip-map" mode.

The look angle and field of view has been tuned to provide optimal resolution and dwell at a flight altitude of 7,000 ft. However, the system will provide retrievals at altitudes ranging from 3,000 feet to the operational ceiling for unpressurised installations at 10,000 feet. The advantage of flying low is to get below the cloud deck while flying high gives more dwell (thus potentially more accurate retrievals).

Direct sun glint can create a problem with wave imaging. The system design has a pair of cameras, one looking forward and one looking backward. This configuration will assure that at least one imager will always be free of sun glint.

Low equipment and operational costs were a system design goal. ROCIS imaging system is comprised of COTS camera and image hardware components. ROCIS can be quickly installed into any survey aircraft with a photogrammetric hole so a dedicated aircraft is not required (**Figure 5**).

The ROCIS imaging system uses a pair of 8-megapixel (3296x2472) panchromatic digital cameras (GiGE model GX3300), each with a 18mm lens (54° x 40° FOV) and a red filter to image the water surface at 2 Hz. The cameras and lens are calibrated for distortion and flat field in the Areté optics laboratory. From 1000m height, the wide field of view translates to an image area on the water that is more than 4 km long. This provides more than 50 seconds of dwell at flight speed of 75 m s^{-1}. Images are recorded to a pair of solid state disk drives with enough storage space to save six hours of continuous 2Hz images from both cameras.

The survey aircraft speeds (~75 m s^{-1}) are one thousand times faster than the slowest ocean currents (~0.05 m s^{-1}) one might want to resolve. This creates a challenge to measure absolute currents. Fortunately, there have been major advances during the past decade in commercial off-the-shelf (COTS) INS.

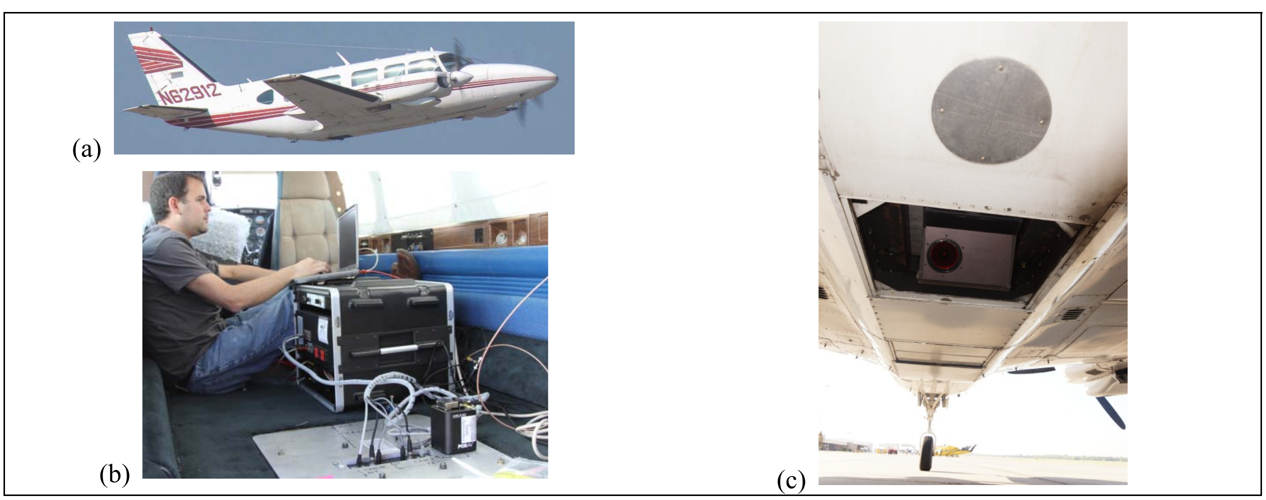

Figure 5. ROCIS imaging hardware. (a) The Navajo Aircraft with the (b) data acquisition computer and INS inside, and (c) the dual cameras installed into the photogrammetric window.

ROCIS uses an Applanix POS-AV 410 INS and Fugro Seastar to provide high accuracy real-time positioning. The POS-AV provides absolute aircraft speed to 0.5 cm s^{-1} and heading drift of less than 0.5° hr^{-1}. This is sufficient to determine absolute current accuracy better than 5 cm s^{-1} with the proposed collection geometry. Boresighting of the INS to the individual cameras is accomplished by flying over and imaging fiducials (targets) with known locations, and determining offset angles through an iterative best fit process.

C. ROCIS Processing Software

The current retrieval processing is conducted after the flight on a ground station computer (an Alienware gaming laptop). The disk drives and INS data are removed from the aircraft and connected to the ground station computer. The software is written in MATLAB and has been optimized for speed.

The operator uses a graphical user interface to select processing parameters including patch size, mapping height and wavenumber band. The operator can select to process the full flight or a sub-region. The software input files include the image files, the INS data, the boresight file and camera calibration files. The software will automatically suggest optimized patch latitude-longitude locations along the flight or the user can select in input file with patch locations.

After software configuration, the automated data processing includes:

- Reading and applying camera calibration to each image
- Matching the image to navigation data
- Mapping the image data to each surface patch within the field of view
- Accumulating time stacks of images for each patch
- Extracting currents from each patch using the 3-D FTT processing
- Saving currents and error metrics for each patch

The data processing is done in stride so each image is only read once from the disk. A cyclical buffer of image time stacks for each patch accumulates mapped image data. When a patch has accumulated enough dwell or is no longer in the field of view, the current retrieval is conducted and that image stack is removed from memory.

Once the processing has begun, it takes approximately one hour of computation to process one hour of flight time for a single row of current vectors every 250m along the flight track. Processing a 3km swath of current vectors (12 current vectors across) takes approximately 10 times longer. The output data is saved to a comma-separated text file.

III. FIELD COLLECTIONS

During October 2012, Areté and Fugro flew a series of ROCIS capability demonstration flights over the Gulf of Mexico. The flight operations were based at Houma–Terrebonne Airport during the week of October 8-12. The ROCIS imaging system was installed on a Piper Navajo at the airport (**Figure 5**). A total of 16 ground targets (fiducials) where laid and surveyed next to the runway.

Skies were partly cloudy every day. We encountered both scattered low (~3000ft) on an inversion layer and high (>15,000 ft) clouds. These clouds were visible in the NOAA Satellite imagery. Over the operational period, the mid-Gulf buoy (NDBC 42001) reported winds ranging from 2 to 10 m s^{-1} out of the northeast, wave heights from 0.5 to 1.7 m and dominate wave periods from 4 to 7 s.

On October 8, we flew an engineering check out flight after system installation. The aircraft imaged the targets at the air field and flew offshore briefly. Offshore flights were conducted on October 9, 10 and 11 and flown at an elevation of 2133m and speed of 72 m s^{-1}. These flights were each around 4.5 hours in duration and covered approximately 1000 km over the ocean. A portion of the October 9 flight was lost to a system bug that was corrected before the next flight. A set of reciprocal flight lines were flown over Vermillion Bay on October 12 and then the system was removed from the aircraft.

Only two people, a pilot and system operator, are required for the flight operations. They are provided with survey way points but also armed with knowledge of where the strongest current might be located. The flight crew did make some way point adjustments during the flight to avoid some cloudy areas.

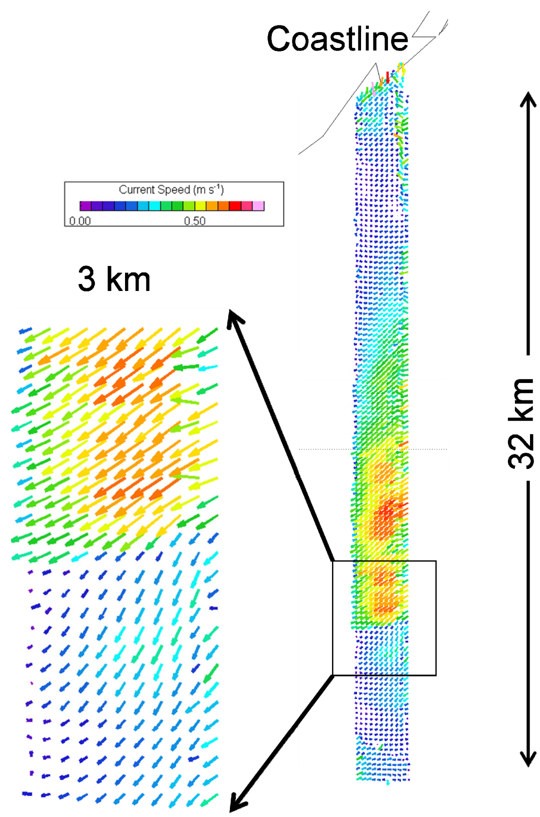

Figure 6. Swath of Current Vectors from Vermillion Bay. The aircraft flew a north to south (NS) route over Vermillion Bay at a speed of 140 knots and altitude of 9000 ft. Current vectors are from a 256m x 256m grid. The cross track swath over vectors 3 km wide is possible because of the imaging system wide field of view. Note the strong velocity front observed.

We determined after the first flight that the camera mount was pitched upward 3 to 5° which placed the nominal look angle for the forward camera closer to the horizon and the aft camera closer to nadir. The pitch was a function of air speed.

Data processing commenced after the aircraft landed and consisted of processing the aft camera for current retrievals every 250m along the flight path. This produced up to 4000 individual current vectors. Plots of current retrieval were produced within 20 hours of the October 9 flight and within 12 hours of the October 10 and 11 flights. Streamlining the operations should get this post-processing down to six hours.

IV. Results

The field collections had two primary goals: (1) quantify the system performance and (2) collect data over operationally relevant regions and conditions.

A. Reciprocal Lines

It is common with boat mounted current meters to conduct reciprocal survey lines to check system calibrations. It is assumed that the ocean currents change slowly in time so that any difference in observed current vectors is indicative of measurement errors. The same thing can be done with ROCIS, with the advantage of the two cameras providing independent information, to check system performance.

On October 12, we flew five reciprocal flights along a 32 km line over Vermillion Bay. Lines consisted of north to south and south to north lines at 2745m (9000ft) and 1825m (6000ft) and one south to north line at 915m. The aircraft speed was 72 m s^{-1}. Currents along this line were calculated in 250m x 250m patches and ranged from 0.05 to 0.7 m s^{-1}. An example of the retrieved currents is shown in **Figure 6**.

To evaluate the system performance, we examined the retrievals from both cameras from the 1825m (6000ft) reciprocal lines (**Figure 7**). The standard velocity was created by averaging all four velocity estimates into 1 km bins. Then the bias and root mean squared (RMS) difference was calculated for each camera and each direction (**Table 1**).

The bias was below 3 cm s^{-1} and the RMS difference was below 4 cm s^{-1}. These differences reflect both errors in the current retrievals and small changes in the ocean currents. Similar results were obtained from the higher and lower flights. These results suggest we met our goal of 5 cm s^{-1} measurement accuracy.

The forward camera current retrievals from the south-north line have the largest errors. Examination of the raw imagery shows some sun glitter on the waves that is not present in the other views. The resulting 3-D PSD exhibits some energy off the dispersion curve which negatively impacted the accuracy to the least squares fit.

Table 1. Observed measurement differences from 1825m (6000ft) reciprocal flight line. Reported values are in cm s^{-1}.

		Bias (cm/s)			RMS Difference (cm/s)		
		Veast	Vnorth	Speed	Veast	Vnorth	Speed
N-S	Aft	0.94	1.39	-1.29	1.34	3.82	2.31
N-S	Fore	0.86	0.17	-1.14	2.02	3.04	2.47
S-N	Aft	0.9	0.92	-1.25	2.61	3.48	2.17
S-N	Fore	-2.25	-2.96	1.36	1.68	3.42	3.94

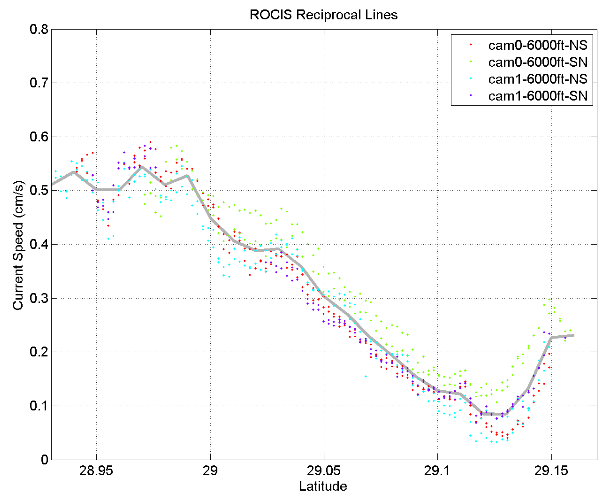

Figure 7. Current Speeds from Reciprocal Flight Lines. The aircraft flew a north to south (NS) route over Vermillion Bay and then turned around and flew the same route in reverse (SN). Cam0 is the aft-looking camera and Cam1 is the forward-looking camera. This provides a total of four samples at each location. The grey line is the averaged current speed from all four observations and smoothed over 1km. The dots are the individual retrievals.

B. Offshore Collections

The offshore collections were designed to sample an operationally relevant region. We identified a Loop Current Eddy (LCE) that we targeted for measurements (see **Figure 8**). This anticyclonic eddy had separated from the Loop Current several months earlier in the year.

We conducted survey flights over this LCE on three consecutive days (October 9, 10 and 11.) The data from consecutive days clearly shows the anticyclonic circulation (**Figure 9**). The strongest currents reached 1.2 m s^{-1} and were observed inside the LCE's western front. Currents inside the eastern front were weaker where the maximum was 0.9 cm s^{-1}. At the center of circulation, the currents dropped to near zero. A persistent near-shore, westward flowing current with maximum speeds 0.6 cm s^{-1} was also observed near Vermillion Bay.

There were few ground truth comparison opportunities offshore. Our flight path included flyovers of two Horizontal Acoustic Doppler Current Profiler installations: #42890 (Murphy Exploration & Production Co. drilling operations) and #42377 (Anadarko Petroleum Corporation), and one DCS Single Current Meter installed on the PAI (Petrobras America

Table 2. Measured currents comparison when ROCIS system passed the ADCPs and PAI DSC.

	Speed (m/s)	Direction (°T)
PAI DSC at 1.5m / ROCIS	0.48 / 0.47	156 / 170
ADCP #42890 at 15.2m / ROCIS	0.32 / 0.32	155 / 160
ADCP #42377 at 21.3m / ROCIS	0.30 / 0.41	143 / 103

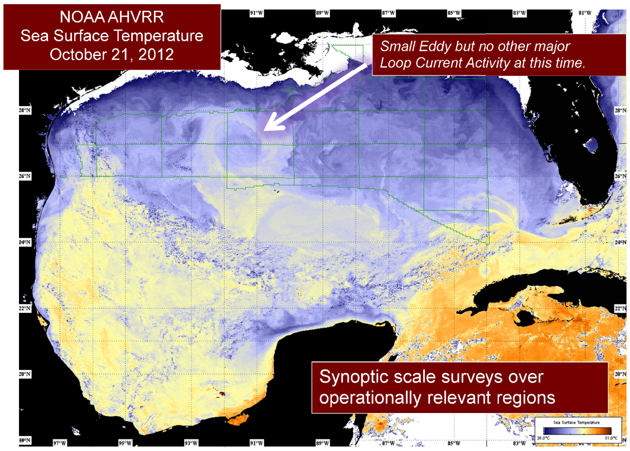

Figure 8. NOAA AVHRR SST. Imagery from October 21, 2012 showing the Loop Current Eddy (LCE) centered at 27°N, 91.5°W.

Inc) deepwater mooring (**Figure 10**). Measurement reporting depth for #42890, #42377 and PAI DCS are 15.2 m, 21.3m and 1.5m respectively. The ADCP and DCS data are 20 minute and 10 minute averages respectively which are compared to a ROCIS current from the nearest 250m x 250m patch.

V. Discussion

The optical remote sensing current measurement technology complements existing measurement systems. During a single six-hour flight, a survey can cover 1,200 km over the region of interest, and yet still provide currents at high resolution and accuracy. This coverage is the clear advantage that ROCIS has over a ship-based current measurement system. However, ROCIS only provides a surface current, so it is not a complete solution to every application.

A survey pattern could be laid out to intensely cover an operational regional in high resolution. Alternately, a survey might aim to capture mesoscale structure such as a Loop Current Eddy (LCE) which would provide insight into its dynamics and be of particular help to both short and long term ocean forecasting.

Although the computational load for the processing is intensive, processing a single flight requires just a few hours to provide operational relevant data. The time required to process current retrievals is nearly the same as the time it takes to collect the data. Therefore, developing a capability that provides current retrievals in real-time (while in the air) is within reach. We hope to demonstrate this capability next year.

A clear downside of optical imaging is that the camera must be able to see the water surface. This means daylight only operations and the atmosphere must be clear of low-clouds and

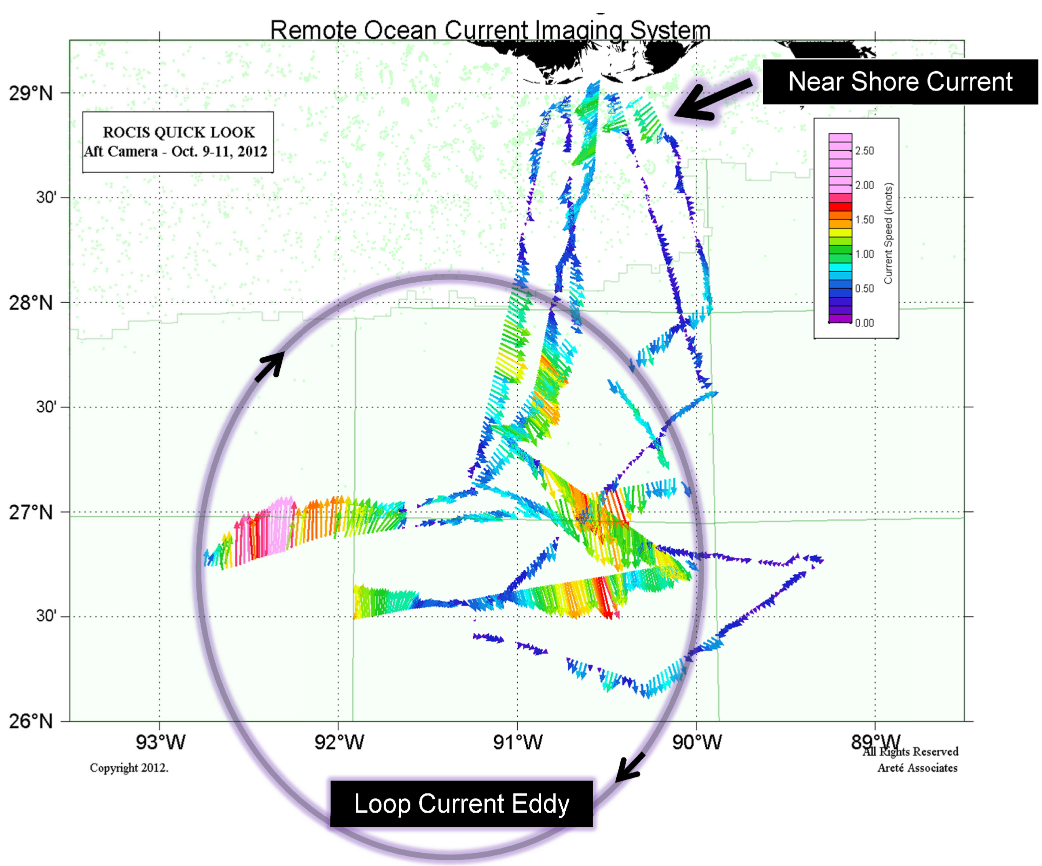

Figure 9. ROCIS Current Measurements. Current vectors were collected during three flights on October 9, 10 and 11. Currents were calculated on 250m x 250m patches along the flight path and then down averaged to every 1 km for plotting.

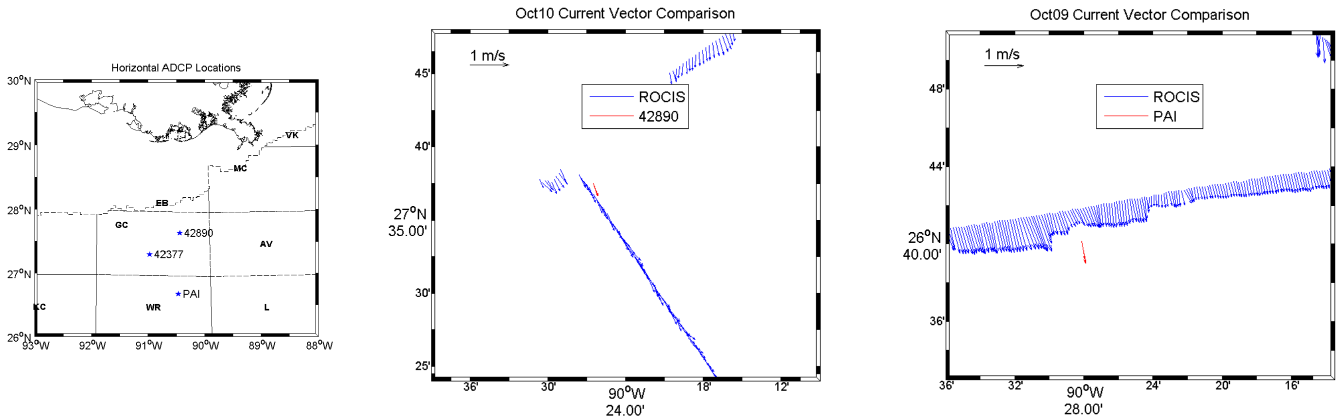

Figure 10. Example Current Measurements Comparison between ROCIS (Blue Arrows) and ADCPs and DSC (Red Arrows).

fog. In practice, the FAA does not recommend small aircraft flying so far offshore at night. We envision that typical operations would require a single survey flight each day. So there may be little practical advantage of using more expensive infrared cameras or active radars. Seeing through clouds would require an active (radar) system. While it is technically possible to measure currents from airborne radar, the hardware and development costs are more expensive and such a system would require a dedicated aircraft. The optical system installations are economical and adaptable to different aircraft.

VI. Conclusions

ROCIS exploits time-space processing of ocean wave imagery to produce maps of surface currents. These results demonstrate that the optical imaging technique has the potential to provide accurate surface current data over large areas both rapidly and cost effectively and complements traditional ocean survey approaches. This unique capability provides maps of current vectors on 250m x 250m (or finer) grids across a 3 km swath along the flight path. The data is suitable for analysis of coherent features, statistical and Fourier analysis, estimation of convergence and vorticity, and assimilation into numerical models. This provides a new tool for studying ocean submesoscale processes.

In catastrophic circumstances, the ROCIS or a similar system would be of value. It could be integrated with multi-spectra and radar oil mapping systems on the same platform. Specifically, with respect to oil spills, the ability to mobilize the system promptly and concentrate data acquisition in specific areas would allow crucial surface current data to be acquired, leading to a significant improvement in the prediction of the path of the spill and thereby enhancing the effectiveness and efficiency of cleanup operations. Additionally, in search and rescue operation, the USCG [13] has determined that access to accurate surface current data improves success rates from 22% to between 48% and 67% representing a value of between $78 and $135 million savings for the United States per annum.

References

[1] W. J. Emery, A. C. Thomas, M. J. Collins, W. R. Crawford, and D. L. Mackas, “An objective method for computing advective surface velocities from sequential infrared satellite images,” J. Geophys. Res., vol. 91, no. C11, pp. 12 865–12 878, 198R.

[2] R. Leben, G. Born and B. Engegreth. "Operational Altimeter Data Processing for Mesoscale Monitoring." Marine Geodesy, 25:3-18, 2002.

[3] Anderson, S. P. and N. Sharma. "Satellite-Tracked Drifter Measurements of Inertial Currents in the Gulf of Mexico." Proceedings of the IEEE Ninth Working Conference on Current Measurement. March, 2008, Charleston, SC. IEEE #1-4244-1486-5/08.

[4] Anderson, S. P., C. K. Cooper, D. B. Driver and J. van Smirren. "EddyNet: A Measurement Program for Collecting Real-Time Current Profiles from the Gulf of Mexico." Proceedings of the IEEE Seventh Working Conference on Current Measurement. 13-15 March 2003, San Diego, CA. IEEE-#0-7803-7813-X/03, 277-280.

[5] D. Barrick, R. Long, C. Whelan, C. Cooper andJ. Abadin. "Advance Warning of Loop Current from Single-Site SeaSonde on Genesis Oil Platform in the Gulf of Mexico." Proc. of the IEEE/OES Eighth Working Conference on Current Measurement Technology, Judith A. Rizoli, Ed., New York, 2005, IEEE.

[6] Anderson, S. P. and P. Matthews. "A Towed 75 kHz ADCP for Operational Deepwater Current Surveys." Proceedings of the IEEE Eighth Working Conference on Current Measurement. July, 2005, Southampton, UK. IEEE #07803-8989-1/05

[7] R. M. Goldstein and H. A. Zebker. "Interferometric Radar Measurement of Ocean Surface Currents." Nature, 328, 707-709., 1987.

[8] S. J. Frasier and A. J. Camps. "Dual-Beam Interferometry for Ocean Surface Current Vector Mapping." IEEE. Trans. Geos. And Remote Sensing, Vol. 39 (2), 401-414, 2001.

[9] Applanix POS-AV system specifications. http://www.applanix.com/products/airborne/posav.html

[10] J.P. Dugan and C.C. Piotrowski, “Surface current measurements using airborne visible image time series,” Rem. Sens. Environ., 84 (2): 309-319. 2003.

[11] C.C. Piotrowski and J.P. Dugan, “Accuracy of bathymetry and current retrievals from airborne optical time series imaging of shoaling waves,” IEEE Trans. Geoscience and Remote Sensing, vol. 40, pp. 2606-2618, 2002.

[12] J.P. Dugan and C.C. Piotrowski. "Estuarine Flows Measured from an Aircraft. IEEE 8th Current Measurements Technology Conference, Southampton, UK. 2005.

[13] Allen, A. SAROPS: Environmental Data Sources and their Uncertainties. Powerpoint presentation, 2007.